

Evaluation Platform of Gait Rhythm in Relation to Movement Disorder and Sensorimotor Interaction

Leo Ota^{1†}, Ken-ichiro Ogawa¹, Miao Sin Robin Yap¹, and Yoshihiro Miyake¹

¹Department of Computational Intelligence and Systems Science, Tokyo Institute of Technology, Yokohama, Japan
(Tel : +81-45-924-5656; E-mail: ohta@myk.dis.titech.ac.jp, ogawa@dis.titech.ac.jp, robin@myk.dis.titech.ac.jp, miyake@dis.titech.ac.jp)

Abstract: The gait rhythm always fluctuates with time. The purpose of this paper is to construct the evaluation platform of gait rhythm. We focused on the coefficient of variation (CV) and the scaling exponent (α) calculated by detrended fluctuation analysis. The motor symptoms severity of Parkinson's disease was classified. The combination of CV and α has a potential to estimate the severity of a motor symptom (postural instability). In addition, we clarify the effect of relationship between individual gait rhythm and environment rhythm on the individual gait rhythm using rhythmic auditory stimulation. The α tends to be related to stable relationship between gait rhythm and cue rhythm.

Keywords: Gait Rhythm; Scaling Exponent; Coefficient of Variation; Movement Disorder; and Sensorimotor Interaction.

1. INTRODUCTION

Walking is emerged from global entrainment with environment [1]. Rhythm is important in walking because global entrainment with environment can be confirmed by gait rhythm. In healthy young people, gait rhythm fluctuation is small, and gait rhythm time series have long-term persistence [2]. However, the long-term persistence in walking paced by rhythmic auditory stimulation [3], diminished with time.

The gait rhythm fluctuation is altered in Parkinson's disease (PD), too [4]. PD is one of the neurodegenerative diseases which causes movement disorder. One of the main symptoms is postural instability (PI), and it is related to gait disturbances [5].

Rhythmic auditory stimulation (RAS) is one of the methods for gait training using sensorimotor interaction for PD [4,6]. This method suggests that fixed-tempo RAS decreases the coefficient of variation (CV), and interactive RAS improves mainly the scaling exponent α , which represents the fluctuation property of gait rhythm. It is calculated by detrended fluctuation analysis.

However, it is not clear whether CV and α , which evaluate the individual dynamics of gait rhythm, are related to the clinical symptoms and sensorimotor interaction. This study focused on PI as a major clinical symptom in PD patients, and we classify the subjects according to its presence or absence. Further, the severity of PI in a group of PD patients is classified. In addition, we compare healthy young people's walking with different rhythmic cues.

2. METHOD

2.1 Classification of severity of Postural instability

2.1.1 Participants and procedures

The Kanto Central Hospital Ethical Committee approved the procedure of this experiment. Written informed consent was provided to all participants. Forty-five patients with PD and 17 healthy people participated in the experiment. All patients walked about 200m once. Participants were divided into 4 groups (see Table 1). We focused on the postural instability (PI) as a

major motor symptom seen in PD and modified Hoehn and Yahr scale (H&Y) was used to determine the absence or presence of PI, and whether mild or obvious PI is observed [7-9]. Performance on the pull test is included in check item of H&Y. PI can be classified by the performance of the pull test; H&Y 2 or less with no sign of PI (no-PI), H&Y 2.5 with signs of mild PI (mild-PI), and H&Y 3 with obvious signs of PI (obvious-PI).

2.1.2 Data acquisition and statistical analysis

Foot contact timings were sensed by foot switches (OT-21BP-G, Ojiden, Japan), and sent to a laptop PC (CF-W5AWDBJR, Panasonic, Japan) by wireless transmitter (S-1019M1F, Smart Sensor Technology, Japan). The stride interval $u_h(t)$ is described as

$$u_h(i) = t_h(i+1) - t_h(i) \quad (1)$$

where $t_h(i)$ is the i -th step timing of the subjects' same leg.

CV is calculated as the standard deviation divided by average. The larger the fluctuation, the larger the CV.

We focused on α to evaluate the persistence in gait rhythm. α can be quantified by detrended fluctuation analysis (DFA) [10,11] based on the following calculation.

$$y_k = \frac{1}{N} \sum_{j=1}^k [u(j) - \langle u \rangle] \quad (2)$$

$$F(n) = \sqrt{\frac{1}{N'} \sum_k [y(k) - y_n(k)]^2} \propto n^\alpha \quad (3)$$

Table 1. Characteristics of participants in 4 groups.

| Group | PI (n = 26) | no-PI (n = 36) | p | obvious-PI (n = 15) | mild-PI (n = 11) | P |
|-----------------|----------------|-------------------|------|------------------------|---------------------|------|
| Mean age (year) | 72.7 | 68.1 | 0.01 | 73.0 | 72.3 | 0.83 |
| H&Y (range) | 2.5 - 3 | Healthy & 1 - 2 | - | 3 | 2.5 | - |

p - values were based on Welch's two sample t -test.

[†] Leo Ota is the presenter of this paper.

where n is a box size, $y_n(k)$ is local trend in each box ($k = 1, \dots, N'$) and $N' = \lfloor N \rfloor$. If α is near 0.5, the time series is white noise. If α is near 1.0, the time series has long-term persistence.

Support vector machine was used with a combination of CV and α to obtain a function for dividing the measured data into two groups [12,13]. CV and α were normalized. One of the soft margin support vector machine, C-SVM was used. The advantage of SVM is easily extended to the nonlinear discriminant analysis by using a nonlinear kernel. At first, we classified the difference between presence and absence of postural instability (PI). Then we focused on people with PI, and classified the difference between mild PI and obvious PI. For preprocessing, we standardize each CV and α value by setting minimum value to 0 and maximum value to 1, in order to eliminate the effect of difference of variation in each scale. The algorithm of SVM is summarized below.

Ordered pair was determined as follows:

$$(\mathbf{x}_1, y_1), \dots, (\mathbf{x}_l, y_l) \in \mathbf{R}^N \times \{-1, 1\} \quad (4)$$

where \mathbf{x}_i is the data vector and y_i is the pair of CV and α , label y_i is the group ID which is related to the score of H&Y, and l is the number of the training data. The classifier determines the hyperplane based on certain optimization criteria. At first, the model is trained by using data. Then we estimate the accuracy by using the test data. We use the leave-one-out method to estimate the accuracy of the classification. In this method, data were divided into two parts, namely test data and training data. The accuracy is estimated by the accurate rate for all combination of test data and training data. In the test phase, the label for test data is determined by the sign of $f(x)$ defined by

$$f(x) = \omega \cdot x + b \quad (5)$$

By margin maximization criterion, a hyperplane is determined uniquely and described by the support vectors, i.e. the nearest data to the hyperplane. The solution to this hyperplane is formulated by

$$\text{minimize } \frac{1}{2} \|\omega\|^2 + C \sum_i \xi_i \quad (6)$$

$$\text{s.t. } y_i(\omega x_i + b) \geq 1 - \xi_i, \quad \xi_i > \forall i \quad (7)$$

where ξ_i is a slack variable, and the value of C corresponds to the size of penalty which is imposed when the value is against the constraints. To solve this problem, (6) is deformed to (8) using Lagrange multipliers α_i ,

$$L_D = \sum_{i=1}^l \alpha_i - \frac{1}{2} \sum_{i=1}^l \sum_{j=1}^l \alpha_i \alpha_j y_i y_j (\mathbf{x}_i \cdot \mathbf{x}_j) \quad (8)$$

$$\text{s.t. } 0 \leq \alpha_i \leq C, \sum_i \alpha_i y_i = 0 \quad (9)$$

From the comparison between expressions in (5) and (8), ω is regarded as the left-hand side of

$$\omega = \sum_{i=1}^{N_s} y_i \alpha_i \mathbf{x}_i \quad (10)$$

where N_s is the number of support vector. By substituting (10), equation (5) is deformed as

$$f(x) = \sum_{i=1}^{N_s} y_i \alpha_i (x \cdot \mathbf{x}_i) + b \quad (11)$$

Then, the inner product $(x \cdot \mathbf{x}_i)$ is substituted for the

symmetrical kernel function $K(x \cdot \mathbf{x}_i)$. This approach is known as the kernel trick. This replacement is equivalent to the inner product after the implicit mapping $\phi(x)$, as shown in

$$K(x \cdot \mathbf{x}_i) = \phi(x) \cdot \phi(\mathbf{x}_i) \quad (12)$$

Here the explicit form of $\phi(x)$ is not required in the calculation of $K(x \cdot \mathbf{x}_i)$.

By replacing $(x \cdot \mathbf{x}_i)$ with $K(x \cdot \mathbf{x}_i)$, equation (11) is reformed to

$$S(x) = \sum_{i=1}^{N_s} y_i \alpha_i K(x \cdot \mathbf{x}_i) + b \quad (13)$$

Then non-linear discriminant function $S(x)$ is determined. In this study, the radial basis function (RBF) kernel was used.

$$K(x \cdot \mathbf{x}_i) = \exp(-\gamma \|x - \mathbf{x}_i\|^2) \quad (14)$$

Here the parameter of RBF kernel and the parameter of C-SVM is related to the large effects on the classification results. Parameters γ and C were optimized using grid search. The search area was [0.001, 1000]. Leave-one-out method was used to estimate the accuracy. Then we determined the combination of C and γ as the values minimize the classification accuracy.

2.2 Effect of individual phase or phase frequency difference to environment

2.2.1 Participants and procedures

In addition, 5 healthy young people (age: 24-28 years old; 5 male) participated in the experiment. All healthy young participants walked following the rhythmic auditory cue, which was provided after first 20 s. In step-sound condition, auditory cue is provided when foot contact was detected. In slow-tempo, similar-tempo, and fast-tempo conditions, the mean value of first 5 stride intervals of both legs (maximum and minimum value were eliminated.) was calculated as baseline, and rhythmic cue tempo was set to 70%, 100%, or 130%. Each trial contains over 120 strides, and first 20 strides and last 10 strides were not analyzed to eliminate the transient phase.

2.2.3 Data acquisition and statistical analysis

Foot contact timings were sensed by the same system as described in 2.1.2.

The subject's stride interval $u_h(t)$ is described in (1). This equation is also applicable to rhythmic cues, after replacing the suffix h (for human) with cue (for cue).

CV and α of stride interval are used to evaluate the individual gait dynamics. To check whether gait rhythm can be entrained to cue rhythm, we calculate the mean value of each participant's stride interval.

To confirm the relationship between gait rhythm phase and cue rhythm phase, circular variance V can be calculated by following Eqs. (15)-(17) [14].

$$\Delta\theta_i = \{t_{cue}(i) - t_h(i)\} \frac{2\pi}{u_h(i)} \quad (15)$$

$$Re^{i\theta} = \frac{1}{N} \sum_j e^{i\Delta\theta_j} = \langle e^{i\Delta\theta_j} \rangle \quad (16)$$

$$V = 1 - R \quad (0 \leq V \leq 1) \quad (17)$$

where $\Delta\theta_j$ is the j -th phase difference between j -th human foot contact and j -th auditory cue ($j = 1, \dots, N$), and N is the data length. V can quantify the relationship

between human gait rhythm and cue rhythm, and it estimate the entrainment between human foot steps and rhythmic cue. The larger the circular variance V is, the smaller the value R is, and vice versa.

3. RESULTS AND DISCUSSION

3.1 Results of classification of severity of movement disorder as an individual control disorder

At first, we classify the patients into PI and no-PI. Figure 1 shows the result of grid search to find optimized parameter pairs of C and γ . The best error rate was 25% at combination of $C=1$, and $\gamma=1$. Figure 2 shows the result of the classification of presence or absence of PI in the plane configured by CV and α . The accuracy was 74%.

Then we classify the patients with PI into obvious-PI and mild-PI. Figure 3 shows the result of grid search to find optimized parameter pair of C and γ in classification between obvious-PI and mild-PI. The best error rate with the smallest value 23% at optimized combination of C and γ was $C=1$, $\gamma=0.1$. Figure 4 shows the result of the classification of severity difference of PI in the plane configured by CV and α . The accuracy was 77%.

These results suggest that the combination of CV and α can differentiate between PI and no-PI, and between obvious-PI and mild-PI using nonlinear method. However, there are misclassification, and the reason may be due to the overlap between the two classified distributions. It is possible to improve the classification accuracy by adding new features.

3.2 Effect of self-paced walking or paced walking on individual gait dynamics

Samples of stride interval data of healthy young person were shown in Fig. 5. CV in step-sound condition (Fig. 5A) was the same as similar-tempo condition (Fig. 5B). However, α in step-sound condition was higher than similar-tempo condition. The circular variance of phase difference was relatively small.

Table 2 shows the results of the experiment of healthy young participants' walking with rhythmic auditory cue. Mean stride interval in slow-tempo and similar-tempo condition were different from step-sound condition. However, phase difference in step-sound condition was

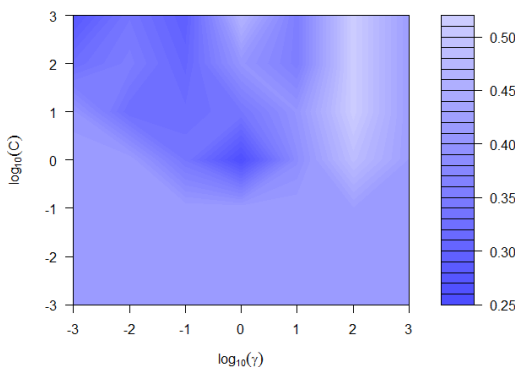


Fig.1 Performance of SVM in classification of presence or absence of postural instability. The colors represent the error rate of classification.

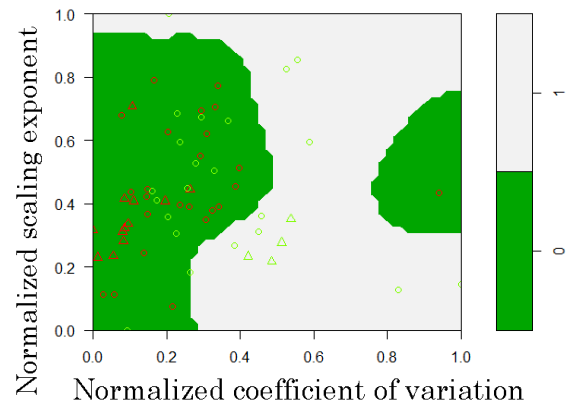


Fig.2 Result of SVM on the plane configured by CV and α . The colors of markers show the group label of the data for training; red: no-PI, light green: PI (postural instability). Shape of marker shows whether the data is support vector or not; circle: support vector, triangle: others. Background color shows the predicted label of the tested data (green = 0: no-PI, white = 1: PI).

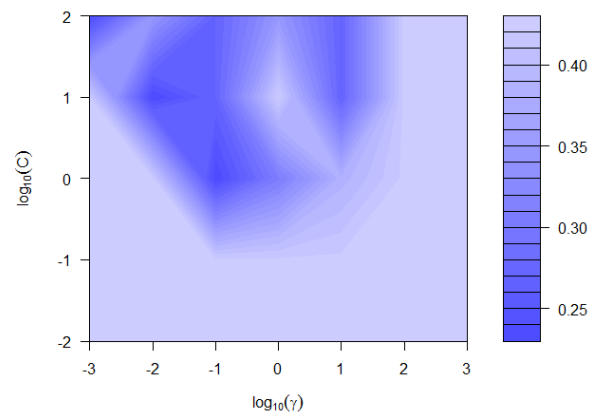


Fig.3 Performance of SVM in classification between mild and obvious postural instability. The colors represent the error rate of classification.

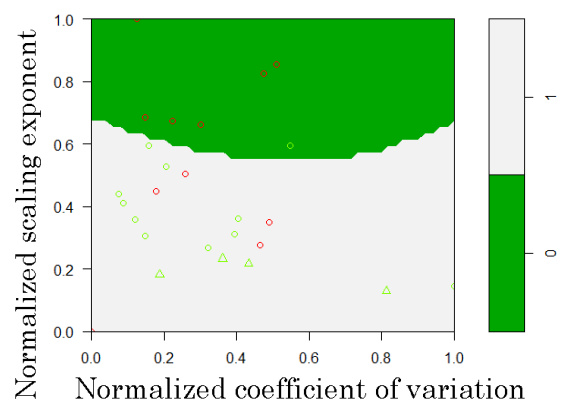


Fig.4 Result of SVM on the plane configured by CV and α . The color of markers show the group label of the data for training (red: mild-PI, light green: obvious-PI). Shape of marker shows whether the data is support vector or not; circle: support vector, triangle: others. Background color shows the predicted label of the tested data (green = 0: mild-PI, white = 1: obvious-PI).

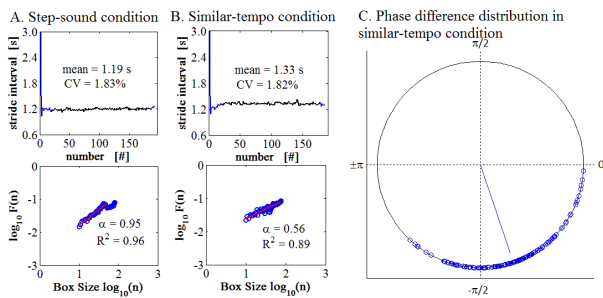


Fig.5 Samples of stride interval and phase difference distribution of healthy young person.

Table 2. Comparison of stride interval and phase difference between step-sound and fixed-tempo conditions (n=5).

| | Step sound | Slow tempo | Similar tempo | Fast tempo | <i>p</i> |
|-------------------|------------|------------|---------------|------------|----------|
| Mean [s] | 1.13 | 1.87* | 1.50* | 1.11 | <0.01 |
| CV [%] | 2.8 | 4.0 | 2.6 | 2.9 | 0.34 |
| α | 0.88 | 0.50* | 0.45* | 0.51* | 0.04 |
| Circular variance | 0 | 0.33* | 0.21* | 0.25* | 0.03 |

*: statistical difference from step-sound condition (significant level: $p < 0.05$, Holm's adjustment method were used). †: statistical different tendency from step-sound condition (significant level: $p < 0.10$, Holm's adjustment method were used). *p* - values were based on Kruskal-Wallis rank sum test.

obviously different from other conditions. Significant difference of CV among 4 conditions was not observed but α in step-sound condition was significantly different from other conditions. This suggests that α can be related to the distribution of phase difference.

These results were for healthy young people. Healthy young people's gait dynamics is different from PD patients or elderly people [4]. However, Hove et al. reported that $1/f$ fluctuation property, which is related to long term persistence, were reinstated by interactive rhythmic auditory stimulation (RAS), not by fixed-tempo RAS [6]. Circular variance of phase difference between step and cue is converged rapidly by interaction between human rhythm and cue rhythm. Therefore, the interactivity between human and environment might be essential for considering rehabilitation methodology.

Consequently, the combination of CV and α has a potential to evaluate movement disorders or rehabilitation using sensorimotor interaction.

ACKNOWLEDGEMENT

I would like to thank Doctor Satoshi Orimo from Kanto Central Hospital for his assistance in introducing PD patients. I am also grateful to patients from Kanto Central Hospital for their participation in this experiment.

REFERENCES

- [1] G. Taga, "A model of the neuro-musculo-skeletal system for human locomotion", *Biological Cybernetics*, Vol. 73, pp. 97-111, 1995.
- [2] J. M. Hausdorff, P. L. Purdon, C.-K. Peng, Z. Ladin, J. Y. Wei, and A. L. Goldberger, "Fractal dynamics of human gait: stability of long-range correlations in stride interval fluctuations", *Journal of Applied Physiology*, Vol. 80, No. 5, pp. 1448-1457, 1996.
- [3] D. Delignieres, and K. Torre, "Fractal dynamics of human gait: a reassessment of the 1996 data of Hausdorff et al.", *Journal of Applied Physiology*, Vol. 106, pp. 1272-1279, 2009.
- [4] J. M. Hausdorff, "Gait dynamics in Parkinson's disease: Common and distinct behavior among stride length, gait variability, and fractal-like scaling", *Chaos*, Vol. 19, 026113, pp. 1-9, 2012. doi: 10.1063/1.3147408.
- [5] J. Jankovic, "Parkinson's disease: clinical features and diagnosis", *J Neurol Neurosurg Psychiatry*, Vol. 79, pp. 368-376, 2008. doi:10.1136/jnnp.2007.131045
- [6] M. J. Hove, K. Suzuki, H. Uchitomi, S. Orimo, and Y. Miyake, "Interactive rhythmic auditory stimulation reinstates natural $1/f$ timing in gait of Parkinson's patients", *PLoS ONE* Vol. 7, e32600, 2012.
- [7] M. M. Hoehn and M. D. Yahr, "Parkinsonism: onset, progression, and mortality.", *Neurology*, vol. 17, no. 5, pp. 427-442, 1967.
- [8] C. G. Goetz, W. Poewe, O. Rascol, C. Sampaio, G. T. Stebbins, C. Counsell, N. Giladi, R. G. Holloway, C. G. Moore, G. K. Wenning, M. D. Yahr, and L. Seidl, "Movement Disorder Society Task Force Report on the Hoehn and Yahr Staging Scale : Status and Recommendations," *Movement Disorders*, vol. 19, no. 9, pp. 1020-1028, 2004.
- [9] L. Ota, K. Ogawa, S. Orimo, Y. Miyake, "Relation of postural instability to gait dynamics in patients with Parkinson's disease", *Proc. of 2014 ICME International Conference on Complex Medical Engineering*, pp.195-200, 2014.
- [10] C. K. Peng, S. V. Buldyrev, S. Havlin, M. Simons, H. E. Stanley, et al. Mosaic organization of DNA nucleotides. *Phys Rev E Stat Phys Plasmas Fluids Relat Interdiscip Topics* 49, pp.1685-1689, 1994.
- [11] C.-K. Peng, S. Havlin, H. E. Stanley, and A. L. Goldberger, "Quantification of scaling exponents and crossover phenomena in nonstationary heartbeat time series", *Chaos*, Vol. 5, pp. 82-87, 1995.
- [12] Vapnik, V. (1995). *The nature of statistical learning theory*. Berlin: Springer.
- [13] A. Karatzoglou, D. Meyer, and K. Hornik, Support vector machines in R," *Biological Cybernetics*, vol.15, no.9, pp.147-159, 2006.
- [14] N. I. Fisher, "Statistical analysis of circular data", *Cambridge University Press*, Cambridge, 1993.